Published in final edited form as:
Cancer Res. 2011 March 1; 71(5): 1573–1583. doi:10.1158/0008-5472.CAN-10-3126.

Reduced VEGF production, angiogenesis, and vascular regrowth contribute to the antitumor properties of dual mTORC1/mTORC2 inhibitors

Beverly L. Falcon[1,*], **Sharon Barr**[2,*], **Prafulla C. Gokhale**[2], **Jeyling Chou**[1], **Jennifer Fogarty**[1], **Philippe Depeille**[1], **Mark Miglarese**[2], **David M. Epstein**[2], and **Donald M. McDonald**[1]

[1] Cardiovascular Research Institute, Comprehensive Cancer Center, and Department of Anatomy, University of California, San Francisco, California, USA

[2] OSI Pharmaceuticals, Inc., Farmingdale, New York, USA

Abstract

The mammalian target of rapamycin (mTOR) pathway is implicated widely in cancer pathophysiology. Dual inhibition of the mTOR kinase complexes mTORC1 and mTORC2 decreases tumor xenograft growth in vivo and VEGF secretion in vitro, but the relationship between these two effects are unclear. In this study, we examined the effects of mTORC1/2 dual inhibition on VEGF production, tumor angiogenesis, vascular regression, and vascular regrowth, and we compared the effects of dual inhibition to mTORC1 inhibition alone. ATP-competitive inhibitors OSI-027 and OXA-01 targeted both mTORC1 and mTORC2 signaling in vitro and in vivo, unlike rapamycin which only inhibited mTORC1 signaling. OXA-01 reduced VEGF production in tumors in a manner associated with decreased vessel sprouting but little vascular regression. In contrast, rapamycin exerted less effect on tumoral production of VEGF. Treatment with the selective VEGFR inhibitor OSI-930 reduced vessel sprouting and caused substantial vascular regression in tumors. However, following discontinuation of OSI-930 administration tumor regrowth could be slowed by OXA-01 treatment. Combining dual inhibitors of mTORC1 and mTORC2 with a VEGFR2 inhibitor decreased tumor growth more than either inhibitor alone. Together, these results indicate that dual inhibition of mTORC1/2 exerts anti-angiogenic and anti-tumoral effects that are even more efficacious when combined with a VEGFR antagonist.

Keywords

mTOR; VEGF; angiogenesis; vascular regrowth; RIP-Tag2 tumors

Introduction

The mammalian target of rapamycin (mTOR), a serine/threonine kinase, integrates multiple signaling pathways, including cell growth and survival. mTOR exists in two complexes, mTORC1 and mTORC2. mTORC1 activation through PI3K and Akt controls cell growth by regulating translation, ribosome biogenesis, autophagy, and metabolism (1). While

Address correspondence to: DM McDonald, Department of Anatomy, University of California, 513 Parnassus Avenue, Room S1363, San Francisco, California 94143-0452, USA. Telephone: 415-476-2118; Fax 415-502-0418; donald.mcdonald@ucsf.edu.

*BLF and SB contributed equally to this work

SB, PCG, MM, and DME are employees of OSI Pharmaceuticals

mTORC2 phosphorylates Akt, SGK1, and PKC to control cell survival and cytoskeletal organization (2).

Many mTOR activators and effectors are overexpressed or mutated in cancer (3). Rapamycin and its analogs (rapalogs) are allosteric inhibitors of mTORC1 that are clinically effective in some tumors (3,4). mTORC1 inhibition, however, activates mTORC2 signaling via p70S6K-IRS1 negative feedback, thus limiting the efficacy of rapalogs (5–7). Recent evidence indicates broader and more robust anticancer effects are achieved by inhibiting both mTORC1 and mTORC2 (8–11). Furthermore, mTOR catalytic site inhibitors elicit greater inhibition of mTORC1 activity. Consistent with mTORC2 regulation of Akt, these studies show greater reductions in Akt signaling and tumor cell proliferation by inhibiting both mTORC1 and mTORC2 compared to just mTORC1 (8–11). mTORC1/mTORC2 inhibition also reduces HIF1-alpha expression, vascular endothelial growth factor (VEGF) secretion, and tumor angiogenesis (10,11).

VEGF inhibitors reduce angiogenesis, cause tumor vessel regression, slow tumor growth, and may improve drug delivery (12–15). Despite the well-documented role for VEGF in tumor angiogenesis and growth (16), current approaches block the VEGF ligand or receptor. Little is known about the effects on the tumor vasculature of reducing VEGF production. Although VEGF inhibitors can destroy as much as 80% of the tumor vasculature, most tumor vessels grow back after the treatment ends (17). This vessel regrowth is likely due to continued VEGF production because inhibition of matrix metalloproteinases or type IV collagen cryptic sites does not slow revascularization (17).

Previous studies examined mTORC1/mTORC2 inhibition on VEGF secretion in vitro (11) or rapamycin on tumor vessels in vivo (10,18,19). However, mTORC1/mTORC2 inhibition on tumor vessels and VEGF production *in vivo* has not been studied. We hypothesized that dual mTORC1 and mTORC2 inhibition would provide superior inhibition of Akt signaling and VEGF production and greater effects on tumor cells and tumor vasculature than inhibition of mTORC1 alone. To study this, we used small molecule ATP-competitive inhibitors, OXA-01 and OSI-027. These drugs selectively inhibit both mTORC1 and mTORC2. We compared the effects of these molecules to rapamycin, an allosteric mTORC1 inhibitor. Moreover, we determined if combining mTORC1/mTORC2 and VEGFR inhibition had greater antitumor effects than either inhibitor alone. Our findings indicate that mTORC1/mTORC2 inhibition impacted tumors through two mechanisms: first, direct effects on tumor cells decreased proliferation and increased apoptosis; and second, anti-vasculature effects were more pronounced than after mTORC1 inhibition alone. When dual mTORC1/mTORC2 inhibition was combined with VEGFR inhibition, effects on tumor cell proliferation and apoptosis and on tumor growth were even greater. Together, these results support the use of mTORC1/mTORC2 inhibitors as monotherapy, as monotherapy alternating with an anti-angiogenic agent, or as combination therapy given concurrently with an anti-angiogenic agent.

Materials and Methods

Biochemical and cellular selectivity assays

mTORC1 and mTORC2 inhibition was assayed using native enzyme complex immunoprecipitated from HeLa lysates at 1mM ATP as described (20). The HTRF assay was used for the PI3K assay (Millipore, MA, USA) and DNA-PK activity was measured using human recombinant p53 protein (Axxora, CA, USA) and phospho-p53 (S15) antibodies (Cell Signaling Technologies, MA, USA). Both assays used 100mM ATP. Panels of additional kinases were assessed for OXA-01 and OSI- 027 selectivity as described in the supplemental methods.

Cell Culture

H292 cells from ATCC were cultured as directed. Ovcar-5 cells, a generous gift of Dr. T. Frederick, were cultured in RPMI plus 10% serum and 1% L-glutamine.

In vivo anti-tumor efficacy studies

For xenograft models, cells were harvested, implanted s.c. in the right flank of nu/nu CD-1 mice and tumor growth was analyzed as described (21,22). Tumor growth inhibition and regression calculations are included in supplemental methods. Tumor samples were collected and snap frozen at specified time points. Tumor lysates were prepared by homogenization (Precellys-24 homogenizer; MO Bio Laboratories, Inc., CA) in lysis buffer (1% Triton X-100, 10% glycerol, 50 mM HEPES (pH 7.4), 150 mM NaCl, 1.5 mM $MgCl_2$, 1 mM EDTA, 10 mM NaF, 1 mM Na_3VO_4 and protease and phosphatase inhibitor cocktails (Sigma, MO)). Phosphorylated and total 4E-BP1, Akt or S6 were quantified by Western blot using MultiGauge software (FujiFilm).

RIP-Tag2 mouse studies

RIP-Tag2 mice were used as described (13,17,23). At 9–10 weeks of age, RIP-Tag2 mice were treated for up to 7 days with vehicle (Labrifil or water); 75 mg/kg OXA-01 BID by gavage; 200 mg/kg OSI-930 QD by gavage; or 20 mg/kg rapamycin QD by ip injection. For vascular regrowth studies, 10-week-old RIP-Tag2 mice were treated with: (a) vehicle for 11 days; (b) OSI-930 for 7 days; (c) OSI-930 for 7 days followed by vehicle for 4 days; (d) OSI-930 for 7 days followed by OXA-01 for 4 days; (e) OSI-930 for 7 days followed by rapamycin for 4 days. Mice used for drug combination studies were treated at doses of 100 mg/kg for OSI-930, 100 mg/kg for OXA-01, and 20 mg/kg for rapamycin, QD for 4 days. During treatments, body weights were monitored daily. If mice lost more than 10% of initial body weight, supplemental fluids were given.

Immunohistochemistry and protein array

Following treatment, RIP-Tag2 mice were fixed by vascular perfusion, tumors were processed for immunohistochemistry, and 60–80 μm sections were stained as described (13,24). Endothelial cells, basement membrane, VEGF, erythrocytes, proliferating and apoptotic cells, and phosphorylated S6K, Akt and 4E-BP1 were identified by immunohistochemistry as described in the Supplementary Methods. VEGF in tumor lysates was performed using mouse angiogenesis arrays (R&D Systems) according to manufacturer's directions.

Microscopy and image analysis

Stained sections of RIP-Tag2 pancreas were examined with Zeiss Axiophot fluorescence and LSM510 laser-scanning confocal microscopes. Area densities were calculated from fluorescence images with ImageJ software (25) using an empirically determined threshold of 30–50 as previously described (13,17,23). Fluorescence intensity was determined as previously described (17) and outlined in detail in the Supplemental Methods. Endothelial sprouts were examined as previously described (24,26).

Statistical analysis

Values expressed as SEM reflect 3–8 mice per group. Significance of differences was determined using ANOVA followed by the Fisher PLSD post-hoc test. For in vivo efficacy studies, rank ANOVA with Dunnett's comparison was used. P values <0.05 were considered statistically significant.

Results

Selectivity of OXA-01 and OSI-027

The goal of this study was to compare dual mTORC1/mTORC2 inhibition on VEGF production, tumor blood vessels, and tumor growth to mTORC1 inhibition alone by rapamycin. To study mTORC1/mTORC2 inhibition, we used selective, ATP competitive inhibitors of the mTOR kinase, OXA-01 and OSI-027. Because these compounds inhibited mTOR kinase activity, each targeted mTORC1 and mTORC2. The IC_{50} for OXA-01 and OSI-027 was 11 nM and 4 nM, respectively (Figure 1). Immunoprecipitation with anti-Raptor antibodies (mTORC1 activity) or anti-Rictor (mTORC2 activity) showed these compounds potently inhibited both mTOR complexes. Greater than 100-fold selectivity was observed for mTOR relative to other PIKK-related kinases in biochemical assays. We also examined OXA-01 and OSI-027 specificity in cell-based assays. OXA-01 and OSI-027 inhibited mTOR signaling of phospho-4E-BP1 with an IC_{50} of 1.1μM and 1μM respectively (Figure 1). Greater than 100-fold selectivity against 37 other protein kinases from tyrosine and serine/threonine families was observed (data not shown). In an assessment of OXA-01 and OSI-027 activity against 98 purified protein kinases, these compounds fully inhibited mTOR. While only 3 kinases were inhibited greater than 90% by OXA-01 and OSI-027: PI3Kδ, PI3Kγ, and RET. JNK3 and MEK2, were inhibited by OXA-01, while PIP5Kγ was significantly inhibited by OSI-027 (data not shown). Both OSI-027 and OXA-01 were inactive against PDK1.

Comparison of OXA-01, OSI-027, and rapamycin on mTORC1/mTORC2 signaling

Effects of OXA-01, OSI-027, and rapamycin on mTORC1 and mTORC2 signaling were compared *in vitro*. OXA-01 or OSI-027, but not rapamycin, dose-dependently attenuated Akt phosphorylation at the mTORC2-specific Ser473 site and the downstream substrate of Akt, PRAS40 (Supplemental Figure 1A). OXA-01 and OSI-027 inhibited 4E-BP1 phosphorylation at Ser37/46, which are typically rapamycin insensitive. Rapamycin failed to inhibit Akt, PRAS40, or 4E-BP1 phosphorylation at these sites, and induced phospho-Akt. Both the mTORC1/mTORC2 inhibitors and rapamycin inhibited S6Kinase and its substrate S6, consistent with mTORC1 regulation of these effectors. Effects of OXA-01, OSI-027, and rapamycin on Akt, 4E-BP1, and S6K phosphorylation was quantified (Supplemental Figure 1B).

In vivo effect of OSI-027, OXA-01 and rapamycin on mTORC1/ mTORC2 signaling and tumor growth

We hypothesized that mTORC1 and mTORC2 inhibition together would slow tumor growth more than mTORC1 inhibition by rapamycin. Effects on GEO colorectal xenograft growth treated with rapamycin (Figure 2A) or OSI-027 (Figure 2B) for 12 days were consistent with our in vitro experiments. Treatment with rapamycin (20 mg/kg) inhibited phospho-S6 and phospho-4E-BP1, while Akt phosphorylation was increased by 29% (Figure 2A). In contrast, OSI-027 (65 mg/kg) inhibited both mTORC1 and mTORC2 effectors. After 2 hours, decreased 4E-BP1, Akt, and S6 phosphorylation was observed and inhibition of S6 and Akt was sustained for 24 hours (Figure 2B). The plasma drug concentration of OSI-027 inversely correlated with these effects on mTORC1 and mTORC2 signaling, and similar pharmacokinetic profiles were observed for OXA-01 (data not shown). The median plasma drug concentration with OSI-027 was 21.3 μM at 2 hours and 14.9 μM at 8 hours. The median plasma concentration of OXA-01 was 25.6 μM at 1 hour and 13.2 μM at 8 hours (data not shown). Consistent with their inhibition of mTORC1 and mTORC2, both OSI-027 (Figure 2C) and OXA-01 (Figure 2D) slowed tumor growth more than did rapamycin.

The effects of mTORC1/mTORC2 inhibition were further compared to mTORC1 inhibition in RIP-Tag2 pancreatic neuroendocrine tumors. Similar to earlier observations, OXA-01 decreased Akt and 4E-BP1 phosphorylation, while rapamycin-mediated inhibition of either effector was not observed (Figure 3A, B). In contrast, both OXA-01 and rapamycin treatment inhibited phopsho-S6K, relative to control (Supplemental figure 2). As indicated by reduced tumor growth in xenograft models, OXA-01 treatment decreased cellular proliferation determined by phospho-histone H3 (Figure 3C) and increased apoptosis measured by activated-caspase-3 (Figure 3D).

Comparison of OXA-01 or rapamycin on VEGF in RIP-Tag2 tumors

Reduced 4E-BP1 phosphorylation at residues T37, T46, S65, and T70 decreases cap-dependent protein translation (27). Because OXA-01 and OSI-027 inhibited rapamycin-resistant sites on 4E-BP1, we hypothesized that OXA-01 treatment would reduce VEGF production more than rapamycin. RIP-Tag2 tumors have high VEGF expression, and the vasculature is sensitive to VEGF inhibition (13), making the model suitable to evaluate the effects of mTOR inhibition on VEGF production and downstream changes in tumor vessels. After treatment with vehicle for 7 days, tumor cells and tumor vessels had intense and roughly equal levels of VEGF immunoreactivity (Figures 4A–B). VEGF staining in tumor vessels had a diffuse component and a punctate component. VEGF immunofluorescence was conspicuously less in both tumor cells and vessels after OXA-01 for 7 days, but the reduction in tumor cells was greater, as evidenced by the persisting pattern of vascular staining (Figure A–B). After rapamycin, VEGF staining was slightly less than baseline, and the reduction was more in tumor cells than in vessels (Figure 4A–B). Overall VEGF fluorescence of entire tumors was reduced by 12%, 48%, and 45% after OXA-01 for 1, 4 or 7 days and only 21% after rapamycin for 7 days (Figure 4C, left). VEGF fluorescence intensity associated with tumor cells was reduced by 65% after OXA-01 for 7 days and was reduced only 34% after rapamycin. VEGF fluorescence associated with tumor vessels was reduced by 48% after OXA-01 but only by 20% after rapamycin (Figure 4C, right).

VEGF expression was also measured in RIP-Tag2 tumors using a multiplex antibody array. Densitometric analysis showed 72% less VEGF-A after OXA-01, but no significant reduction after rapamycin (Figure 4D). VEGF-B expression was unchanged by either treatment (data not shown). The differences in VEGF reductions identified by immunohistochemistry (Figure 4C) and immunoprecipitation (Figure 4D) are likely to reflect the sensitivity of the assays, but both assays showed significantly less VEGF after OXA-01 than after rapamycin.

Effect of OXA-01, rapamycin, and OSI-930 on the tumor vasculature

Because VEGF is important for tumor angiogenesis, we determined whether the decrease in VEGF after OXA-01 or rapamycin reduced RIP-Tag2 tumor vascularity and compared the effect to a VEGFR tyrosine kinase inhibitor, OSI-930 (28). CD31-positive tumor blood vessels were abundant in untreated RIP-Tag2 tumors (Figure 5A). Treatment with OXA-01 for 7 days reduced tumor blood vessels slightly. Rapamycin did not noticeably reduce tumor vascularity, but OSI-930 for 7 days was associated with a large reduction. After OXA-01, tumor vascularity was not detectably reduced at 1, 2, or 4 days but was reduced by 23% at 7 days, compared to baseline. Tumor vascularity was not significantly reduced after rapamycin, but was reduced by 61% after OSI-930 for 7 days (Figure 5B). After VEGF signaling inhibition in tumors, empty basement membrane sleeves can be used as an indication of vessel regression (17,26). Basement membrane sleeves were not apparent after vehicle, OXA-01, or rapamycin, but were numerous after OSI-930 for 7 days (Figure 5C). As an indication of effect on angiogenesis in tumors, the number of vascular sprouts was

reduced by 54% after OXA-01, 21% after rapamycin, and 61% after OSI-930, in comparison to untreated tumors (Figure 5D).

Effect of OXA-01 and rapamycin on vascular regrowth

VEGF inhibition causes tumor vessel regression, but vessel regrowth occurs rapidly after treatment ends (17). Because OXA-01 reduced VEGF and vascular sprouting, we asked whether OXA-01 or rapamycin could prevent vascular regrowth after cessation of VEGFR inhibition by OSI-930. RIP-Tag2 mice were treated with OSI-930 for 7 days, followed by 4 days of treatment with vehicle, OXA-01, or rapamycin. The 4-day time point was chosen because after OXA-01 for 4 days, VEGF was significantly reduced but tumor vascularity was unchanged (Figures 4C and 5B). OSI-930 for 7 days reduced tumor vascularity by 63%, consistent with our previous observations. Four-days after cessation of OSI-930, tumors treated with vehicle exhibited only an 18% decrease in vessel density. Tumors treated with OXA-01 for 4 days after withdrawal of OSI-930 had 40% fewer tumor vessels, but tumors treated with rapamycin were equivalent to vehicle-treated controls (15% reduction) (Figure 6A). Tumors treated with OXA-01 for 1 day after withdrawal of OSI-930, however, had no significant decrease in tumor vessel regrowth, which fit with our finding that OXA-01 for 1 day was insufficient to reduce VEGF (data not shown).

Because VEGF promotes tumor angiogenesis and vascular leakage, we asked whether reductions in VEGF with OXA-01 or rapamycin affected intratumoral hemorrhage assessed by an erythrocyte marker, TER-119. Treatment with OSI-930 for 7 days reduced TER-119 immunoreactivity in RIP-Tag2 tumors by 72%, indicative of a reduction in hemorrhage (Figure 6B). However, 4 days after cessation of OSI-930, TER-119 levels were within 28% of baseline. In contrast, TER-119 levels in tumors treated with OXA-01 or rapamycin after discontinuation of OSI-930 were 50% or 48% less than baseline.

Effects of mTORC1/2 inhibition in combination with VEGFR inhibition

We hypothesized that combining OSI-930 and OXA-01 would reduce tumor growth to a greater extent than either inhibitor alone through additive effects of targeting tumor vessels with OSI-930 and tumor cells with OXA-01. To evaluate this, we examined OSI-930 plus OXA-01 or rapamycin on proliferation (phospho-histone H3) and apoptosis (activated caspase-3). OSI-930 plus OXA-01 reduced phospho-histone H3 more than OSI-930 plus rapamycin (Figure 7A). In addition, OSI-930 combined with OXA-01 was accompanied by a 700% increase in activated caspase-3, but rapamycin plus OSI-930 had no significant effect (Figure 7B).

The RIP-Tag2 model is useful for evaluating the tumor vasculature, but provides a challenging platform for measuring tumor growth kinetics. To confirm the effects of VEGF inhibition combined with mTORC1/mTORC2 inhibition, we used human tumor xenograft models. Because VEGF inhibitors combined with mTOR catalytic site inhibitors could be an option for clinical trials, we used sunitinib, a multi-targeted VEGFR2 inhibitor approved for use in the clinic, with OSI-027, which is in clinical trials. Sunitinib has similar selectivity profiles and equivalent potency for VEGFR2 as OSI-930. Both OSI-930 and sunitinib have a biochemical IC_{50} for VEGFR2 of 9 nM (28–30). Furthermore, OXA-01 plus OSI-930 was not well-tolerated in rodent models for long-term treatment, but no toxicity was found with the OSI-027 and sunitinib combination. The *in vivo* efficacy of OSI-027 plus sunitinib was tested in H292 human lung and Ovcar-5 human ovarian xenograft tumors. H292 tumors, treated with OSI-027 (50 mg/kg) for 21 days had 61% median tumor growth inhibition for the duration of treatment (TGI). Sunitinib (40 mg/kg) for 21 days had 47% median TGI. Combining OSI-027 with sunitinib, however, had a median TGI of 100% with 59% maximal tumor regression (Figure 7C), a statistically significant improvement over either agent alone.

Ovcar-5 xenograft tumors treated with OSI-027 or sunitinib had a 55% and 68% median TGI, respectively. OSI-027 administered with sunitinib had a significantly better median TGI of 100% with 38% maximal tumor regression.

Discussion

Differential effects of dual mTORC1/mTORC2 inhibition versus mTORC1 inhibition on tumor cells and tumor vessels were examined in this study. Consistent with previous reports, we found that mTORC1 and mTORC2 inhibition reduced tumor cell proliferation, increased apoptosis, reduced p-S6K, p-Akt and p-4E-BP1 signaling, and decreased tumor growth compared to vehicle or rapamycin treatment (8–11). Thus, mTORC1/mTORC2 inhibition with OSI-027 or OXA-01 provided greater control of tumor cell proliferation and induction of apoptosis than rapamycin. Dual inhibition of mTORC1 and mTORC2 also had greater anti-angiogenic effects than mTORC1 inhibition. OXA-01 reduced VEGF production in RIP-Tag2 tumors more than rapamycin. The reduction in VEGF production was associated with decreased tumor angiogenesis but not tumor vessel regression. OXA-01 also reduced vascular regrowth following cessation VEGFR2 inhibition with OSI-930. Finally, combining VEGFR inhibition with mTORC1/ mTORC2 inhibition reduced tumor cell proliferation, stimulated tumor cell apoptosis and reduced tumor growth. Together, these results provide support for clinical development of mTORC1 and mTORC2 inhibitors to be used as single agents, in concurrent combination with anti-angiogenic therapeutics or intercalated with anti-angiogenic therapies in an alternating schedule.

Rapalogs are efficacious in some tumors, but feedback activation may limit clinical usefulness (7,31). We reasoned that inhibition of mTORC1 and mTORC2 together would have greater efficacy than mTORC1 inhibition alone. For these studies we used rapamycin as a selective allosteric inhibitor of mTORC1. While rapalogs (everolimus and temsirolimus) are more frequently used cancer therapeutics, these drugs are mechanistically similar to rapamycin and rapamycin is a well-characterized preclinical tool compound. Compared to rapamycin, we found that mTORC1/mTORC2 inhibition with OXA-01 or OSI-027 produced greater reductions in downstream signaling effectors and had greater anti-tumor efficacy in vivo. The reduction in tumor growth probably resulted from reduction in tumor cell proliferation, but increased apoptosis may contribute to this effect. These results are consistent with greater reductions in cell proliferation after mTORC1/ mTORC2 inhibition (8–11) and increased apoptosis in a subset of cell lines (11).

While rapamycin inhibits mTORC1, with prolonged treatment mTORC2 signaling is reduced in select cell lines, presumably through depletion of mTOR from the Rictor complex (32). However, in this study inhibition of the mTORC2 effector Akt or the rapamycin-insensitive sites on 4E-BP1(37/46) after rapamycin treatment in vivo was not observed. Furthermore, in these studies the maximum tolerable dose of rapamycin (20 mg/kg) was used, which is considerably higher than the correlative clinically-relevant dose in humans (33).

OXA-01 treatment of RIP-Tag2 tumors decreased VEGF content and tumor vessel growth. Previous in vitro studies showed decreased VEGF secretion with rapamycin or dual mTORC1/mTORC2 inhibition (11), suggesting VEGF production is dependent on mTORC1. In our *in vivo* studies, rapamycin modestly reduced VEGF, while a greater reduction was achieved with OXA-01. VEGF production is controlled by cap-dependent and -independent translation (34). While rapamycin represses phosphorylation of S6K and certain sites on 4E-BP1, other 4E-BP1 sites (Thr37 and Thr46) are rapamycin-resistant (35). Therefore, mTORC1/mTORC2 inhibition may more completely inhibit cap-dependent translation to maximize the reduction of VEGF in vivo (11). Because VEGF is dependent on

translational regulation, reductions in VEGF content is likely from decreased protein synthesis, however, reduced storage and secretion are possible.

VEGF was reduced in both tumor cells and in clusters associated with the tumor vasculature. This clustered pattern of VEGF immunofluorescence likely represents internalization of VEGF and VEGFR complexes into endothelial cells, as previously described (36–38). Intracellular VEGF complexes are dependent on Akt activation (37). Thus, decreased VEGF internalization with mTORC1/mTORC2 inhibition may be from both reduced VEGF production and Akt signaling.

Inhibitors of the VEGF receptor (e.g. OSI-930, sunitinib, axitinib) or ligand (e.g. bevacizumab) stop tumor vessel growth and prune existing vessels (39). Here, we show reduced VEGF production with mTORC1/mTORC2 inhibition decreases tumor blood vessel growth, but does not cause vessel regression. In a previous study, tumor blood vessels were reduced when mice were pretreated with a mTORC1/mTORC2 inhibitor prior to injection of tumor cells (10), consistent with the idea that mTORC1/mTORC2 inhibition targets tumor vessel growth. Additional studies showed conditional expression of activated-Akt in endothelial cells leads to large and leaky vessels (18,40). In those studies, rapamycin inhibited tumor vessel growth, possibly indicating different thresholds for rapamycin sensitivity depending on Akt activity.

Interestingly, small reductions in VEGF with rapamycin reduced the reappearance of tumor hemorrhage after cessation of VEGFR inhibition, consistent with rapamycin-mediated reductions in vessel leakiness (18). However, larger reductions in VEGF with OXA-01 treatment, reduced the reappearance of both tumor hemorrhage and tumor vessels. Hemorrhage is an indication of tumor vessel leakiness and blood lakes caused by hemorrhage are a conspicuous feature of RIP-Tag2 pancreatic tumors (41,42). Together, these data suggest small reductions in VEGF prevent tumor vessel leakiness, but greater reductions are necessary to slow blood vessel growth. This defines differential responses of tumor blood vessels dependent on the VEGF concentrations in tumors.

Our data support the use of mTORC1/mTORC2 inhibitors, such as OSI-027 and OXA-01, to treat cancer as a single agent or in combination with anti-angiogenic agents. Sunitinib, an approved multi-targeted kinase inhibitor with potent anti-VEGFR2 activity, has a toxicity profile necessitating a drug holiday between dosing regimens. Vascular regrowth can occur following cessation of VEGFR inhibition during drug holidays (17). Our data indicate that OXA-01 treatment slowed vessel regrowth after discontinuation of VEGFR inhibition. Concurrent treatment of tumor xenografts with OSI-930 and OXA-01 also resulted in significant downregulation of tumor cell proliferation and upregulation of apoptosis. Furthermore, combining sunitinib and OSI-027, provides greater inhibition of tumor growth than either single agent. In human xenografts, a schedule of alternating sunitinib and OSI-027 treatment was tolerable, but did not provide better efficacy than continuous single agent administration. Together, these observations suggest that VEGFR2 and mTORC1/mTORC2 co-inhibition targets both the tumor cells and vasculature, resulting in significant tumor growth inhibition. While the precise mechanism is not clear, we hypothesize that increased hypoxia resulting from VEGFR2 antagonism sensitizes tumor cells to mTORC1/mTORC2 inhibition. Previous studies showed hypoxia-induced VEGF production is attenuated by Akt inhibition but not by rapamycin, suggesting mTORC2/Akt signaling axis as a key effector under hypoxic conditions (43). In addition, hypoxia activation of the mTORC2 effector, Akt, protects cells from apoptosis (44–46). Our data indicates OXA-01 but not rapamycin significantly inhibited Akt, and is a likely mechanism for increased apoptosis and decreased tumor growth following combined VEGFR2 and mTORC1/mTORC1 inhibition.

Rapalogs are approved for treatment of advanced renal cell carcinoma. This study indicates that dual inhibition of mTORC1/mTORC2 has more robust antitumor and antivascular effects compared to mTORC1 inhibition. Together, these results indicate unique, therapeutically relevant properties of OXA-01 and OSI-027 that are applicable for clinical development of these drugs for cancer treatment.

Supplementary Material

Refer to Web version on PubMed Central for supplementary material.

Acknowledgments

Research funding: NIH grants: CA82923 from the NCI; HL24136, HL59157, and HL96511 from the NHLBI; a grant from OSI Pharmaceuticals, and funding from The AngelWorks Foundation.

We thank Douglas Hanahan for RIP-Tag2 mice breeding pairs, Ryan Naylor and Katharine Colton for technical help, and Kathleen Wilson for manuscript review. The authors gratefully acknowledge Andrew Crew, Shripad Bhagwat, Jonathan Pachter, Robert Wild, Andrew Cooke, Mark Bittner, Suzanne Russo, Jennifer Kahler, Yan Yao, Christine Mantis, and Eric Brown for designing and characterizing OSI-027 and OXA-01.

References

1. Guertin DA, Sabatini DM. Defining the role of mTOR in cancer. Cancer Cell. 2007; 12:9–22. [PubMed: 17613433]
2. Dowling RJ, Topisirovic I, Fonseca BD, Sonenberg N. Dissecting the role of mTOR: lessons from mTOR inhibitors. Biochim Biophys Acta. 2010; 1804:433–9. [PubMed: 20005306]
3. Easton JB, Houghton PJ. mTOR and cancer therapy. Oncogene. 2006; 25:6436–46. [PubMed: 17041628]
4. Abraham RT, Gibbons JJ. The mammalian target of rapamycin signaling pathway: twists and turns in the road to cancer therapy. Clin Cancer Res. 2007; 13:3109–14. [PubMed: 17545512]
5. Harrington LS, Findlay GM, Gray A, et al. The TSC1-2 tumor suppressor controls insulin-PI3K signaling via regulation of IRS proteins. J Cell Biol. 2004; 166:213–23. [PubMed: 15249583]
6. Julien LA, Carriere A, Moreau J, Roux PP. mTORC1-activated S6K1 phosphorylates Rictor on threonine 1135 and regulates mTORC2 signaling. Mol Cell Biol. 2010; 30:908–21. [PubMed: 19995915]
7. O'Reilly KE, Rojo F, She QB, et al. mTOR inhibition induces upstream receptor tyrosine kinase signaling and activates Akt. Cancer Res. 2006; 66:1500–8. [PubMed: 16452206]
8. Feldman ME, Apsel B, Uotila A, et al. Active-site inhibitors of mTOR target rapamycin-resistant outputs of mTORC1 and mTORC2. PLoS Biol. 2009; 7:e38. [PubMed: 19209957]
9. Thoreen CC, Kang SA, Chang JW, et al. An ATP-competitive mammalian target of rapamycin inhibitor reveals rapamycin-resistant functions of mTORC1. J Biol Chem. 2009; 284:8023–32. [PubMed: 19150980]
10. Xue Q, Hopkins B, Perruzzi C, Udayakumar D, Sherris D, Benjamin LE. Palomid 529, a novel small-molecule drug, is a TORC1/TORC2 inhibitor that reduces tumor growth, tumor angiogenesis, and vascular permeability. Cancer Res. 2008; 68:9551–7. [PubMed: 19010932]
11. Yu K, Toral-Barza L, Shi C, et al. Biochemical, cellular, and in vivo activity of novel ATP-competitive and selective inhibitors of the mammalian target of rapamycin. Cancer Res. 2009; 69:6232–40. [PubMed: 19584280]
12. Huang J, Frischer JS, Serur A, et al. Regression of established tumors and metastases by potent vascular endothelial growth factor blockade. Proc Natl Acad Sci U S A. 2003; 100:7785–90. [PubMed: 12805568]
13. Inai T, Mancuso M, Hashizume H, et al. Inhibition of vascular endothelial growth factor (VEGF) signaling in cancer causes loss of endothelial fenestrations, regression of tumor vessels, and appearance of basement membrane ghosts. Am J Pathol. 2004; 165:35–52. [PubMed: 15215160]

14. Jain RK. Normalization of tumor vasculature: an emerging concept in antiangiogenic therapy. Science. 2005; 307:58–62. [PubMed: 15637262]
15. Tong RT, Boucher Y, Kozin SV, Winkler F, Hicklin DJ, Jain RK. Vascular normalization by vascular endothelial growth factor receptor 2 blockade induces a pressure gradient across the vasculature and improves drug penetration in tumors. Cancer Res. 2004; 64:3731–6. [PubMed: 15172975]
16. Inoue M, Hager JH, Ferrara N, Gerber HP, Hanahan D. VEGF-A has a critical, nonredundant role in angiogenic switching and pancreatic beta cell carcinogenesis. Cancer Cell. 2002; 1:193–202. [PubMed: 12086877]
17. Mancuso MR, Davis R, Norberg SM, et al. Rapid vascular regrowth in tumors after reversal of VEGF inhibition. J Clin Invest. 2006; 116:2610–21. [PubMed: 17016557]
18. Phung TL, Ziv K, Dabydeen D, et al. Pathological angiogenesis is induced by sustained Akt signaling and inhibited by rapamycin. Cancer Cell. 2006; 10:159–70. [PubMed: 16904613]
19. Schnell CR, Stauffer F, Allegrini PR, et al. Effects of the dual phosphatidylinositol 3-kinase/mammalian target of rapamycin inhibitor NVP-BEZ235 on the tumor vasculature: implications for clinical imaging. Cancer Res. 2008; 68:6598–607. [PubMed: 18701483]
20. Bhagwat SV, Kahler J, Yao Y, et al. High-throughput screening for mTORC1/mTORC2 kinase inhibitors using a chemiluminescence-based ELISA assay. Assay Drug Dev Technol. 2009; 7:471–8. [PubMed: 19895344]
21. Buck E, Eyzaguirre A, Rosenfeld-Franklin M, et al. Feedback mechanisms promote cooperativity for small molecule inhibitors of epidermal and insulin-like growth factor receptors. Cancer Res. 2008; 68:8322–32. [PubMed: 18922904]
22. Ji QS, Mulvihill MJ, Rosenfeld-Franklin M, et al. A novel, potent, and selective insulin-like growth factor-I receptor kinase inhibitor blocks insulin-like growth factor-I receptor signaling in vitro and inhibits insulin-like growth factor-I receptor dependent tumor growth in vivo. Mol Cancer Ther. 2007; 6:2158–67. [PubMed: 17671083]
23. Morikawa S, Baluk P, Kaidoh T, Haskell A, Jain RK, McDonald DM. Abnormalities in pericytes on blood vessels and endothelial sprouts in tumors. Am J Pathol. 2002; 160:985–1000. [PubMed: 11891196]
24. Falcon BL, Hashizume H, Koumoutsakos P, et al. Contrasting actions of selective inhibitors of angiopoietin-1 and angiopoietin-2 on the normalization of tumor blood vessels. Am J Pathol. 2009; 175:2159–70. [PubMed: 19815705]
25. Abramoff MD, Magelhaes PJ, Ram SJ. Image Processing with ImageJ. Biophotonics International. 2004; 11:36–42.
26. Hashizume H, Falcon BL, Kuroda T, et al. Complementary actions of inhibitors of angiopoietin-2 and VEGF on tumor angiogenesis and growth. Cancer Res. 2010; 70:2213–23. [PubMed: 20197469]
27. Proud CG. mTOR-mediated regulation of translation factors by amino acids. Biochem Biophys Res Commun. 2004; 313:429–36. [PubMed: 14684180]
28. Garton AJ, Crew AP, Franklin M, et al. OSI-930: a novel selective inhibitor of Kit and kinase insert domain receptor tyrosine kinases with antitumor activity in mouse xenograft models. Cancer Res. 2006; 66:1015–24. [PubMed: 16424037]
29. Mena AC, Pulido EG, Guillen-Ponce C. Understanding the molecular-based mechanism of action of the tyrosine kinase inhibitor: sunitinib. Anticancer Drugs. 2010; 21 (Suppl 1):S3–11. [PubMed: 20110785]
30. Mendel DB, Laird AD, Xin X, et al. In vivo antitumor activity of SU11248, a novel tyrosine kinase inhibitor targeting vascular endothelial growth factor and platelet-derived growth factor receptors: determination of a pharmacokinetic/pharmacodynamic relationship. Clin Cancer Res. 2003; 9:327–37. [PubMed: 12538485]
31. Carracedo A, Pandolfi PP. The PTEN-PI3K pathway: of feedbacks and cross-talks. Oncogene. 2008; 27:5527–41. [PubMed: 18794886]
32. Sarbassov DD, Ali SM, Sengupta S, et al. Prolonged rapamycin treatment inhibits mTORC2 assembly and Akt/PKB. Mol Cell. 2006; 22:159–68. [PubMed: 16603397]

33. Phung TL, Eyiah-Mensah G, O'Donnell RK, et al. Endothelial Akt signaling is rate-limiting for rapamycin inhibition of mouse mammary tumor progression. Cancer Res. 2007; 67:5070–5. [PubMed: 17545582]
34. Braunstein S, Karpisheva K, Pola C, et al. A hypoxia-controlled cap-dependent to cap-independent translation switch in breast cancer. Mol Cell. 2007; 28:501–12. [PubMed: 17996713]
35. Choo AY, Yoon SO, Kim SG, Roux PP, Blenis J. Rapamycin differentially inhibits S6Ks and 4E-BP1 to mediate cell-type-specific repression of mRNA translation. Proc Natl Acad Sci U S A. 2008; 105:17414–9. [PubMed: 18955708]
36. Lampugnani MG, Orsenigo F, Gagliani MC, Tacchetti C, Dejana E. Vascular endothelial cadherin controls VEGFR-2 internalization and signaling from intracellular compartments. J Cell Biol. 2006; 174:593–604. [PubMed: 16893970]
37. Santos SC, Miguel C, Domingues I, et al. VEGF and VEGFR-2 (KDR) internalization is required for endothelial recovery during wound healing. Exp Cell Res. 2007; 313:1561–74. [PubMed: 17382929]
38. You WK, Kasman I, Hu-Lowe DD, McDonald DM. Ricinus communis agglutinin I leads to rapid down-regulation of VEGFR-2 and endothelial cell apoptosis in tumor blood vessels. Am J Pathol. 2010; 176:1927–40. [PubMed: 20185574]
39. Baluk P, Hashizume H, McDonald DM. Cellular abnormalities of blood vessels as targets in cancer. Curr Opin Genet Dev. 2005; 15:102–11. [PubMed: 15661540]
40. Xue Q, Nagy JA, Manseau EJ, Phung TL, Dvorak HF, Benjamin LE. Rapamycin inhibition of the Akt/mTOR pathway blocks select stages of VEGF-A164-driven angiogenesis, in part by blocking S6Kinase. Arterioscler Thromb Vasc Biol. 2009; 29:1172–8. [PubMed: 19443844]
41. Hashizume H, Baluk P, Morikawa S, et al. Openings between defective endothelial cells explain tumor vessel leakiness. Am J Pathol. 2000; 156:1363–80. [PubMed: 10751361]
42. Sennino B, Raatschen HJ, Wendland MF, et al. Correlative dynamic contrast MRI and microscopic assessments of tumor vascularity in RIP-Tag2 transgenic mice. Magn Reson Med. 2009; 62:616–25. [PubMed: 19526501]
43. Kurmasheva RT, Harwood FC, Houghton PJ. Differential regulation of vascular endothelial growth factor by Akt and mammalian target of rapamycin inhibitors in cell lines derived from childhood solid tumors. Mol Cancer Ther. 2007; 6:1620–8. [PubMed: 17483438]
44. Alvarez-Tejado M, Naranjo-Suarez S, Jimenez C, Carrera AC, Landazuri MO, del Peso L. Hypoxia induces the activation of the phosphatidylinositol 3-kinase/Akt cell survival pathway in PC12 cells: protective role in apoptosis. J Biol Chem. 2001; 276:22368–74. [PubMed: 11294857]
45. Beitner-Johnson D, Rust RT, Hsieh TC, Millhorn DE. Hypoxia activates Akt and induces phosphorylation of GSK-3 in PC12 cells. Cell Signal. 2001; 13:23–7. [PubMed: 11257444]
46. Chen EY, Mazure NM, Cooper JA, Giaccia AJ. Hypoxia activates a platelet-derived growth factor receptor/phosphatidylinositol 3-kinase/Akt pathway that results in glycogen synthase kinase-3 inactivation. Cancer Res. 2001; 61:2429–33. [PubMed: 11289110]

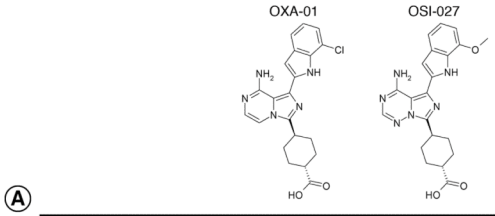

A

B

	Biochemical Selectivity	
In vitro Kinase Assay	OXA-01 IC_{50}, μM	OSI-027 IC_{50}, μM
mTOR kinase	0.011	0.004
mTORC1	0.029	0.022
mTORC2	0.007	0.065
PI3K-α	0.19	1.3
PI3K-β	9.3	>30
PI3K-γ	0.46	0.42
DNA-PK	3.2	1.0

C

	Cellular Selectivity	
Mechanistic Cell Assay	OXA-01 IC_{50}, μM	OSI-027 IC_{50}, μM
mTOR (p4E-BP1)	1.1	1.0
KDR (pVEGFR2)	> 40	> 40
EGFR (pEGFR)	> 40	> 40
EphA2 (pEphA2)	> 40	> 40
SRC (pFAK)	> 40	> 40
MAPK axis (pERK1/2)	> 40	> 20
DNA-PK (pRPA32)	> 40	30
NFkB (p-p65)	> 30	>10

Figure 1. Selectivity of mTORC1/mTORC2 inhibitors, OXA-01 and OSI-027

A Structures for OXA-01 and OSI-027 are shown. **B.** In vitro IC_{50} values for a representative set of kinases are shown. **C.** Selectivity was further demonstrated in cell-based assays using phosphorylated kinases or downstream effectors as a measure of activity.

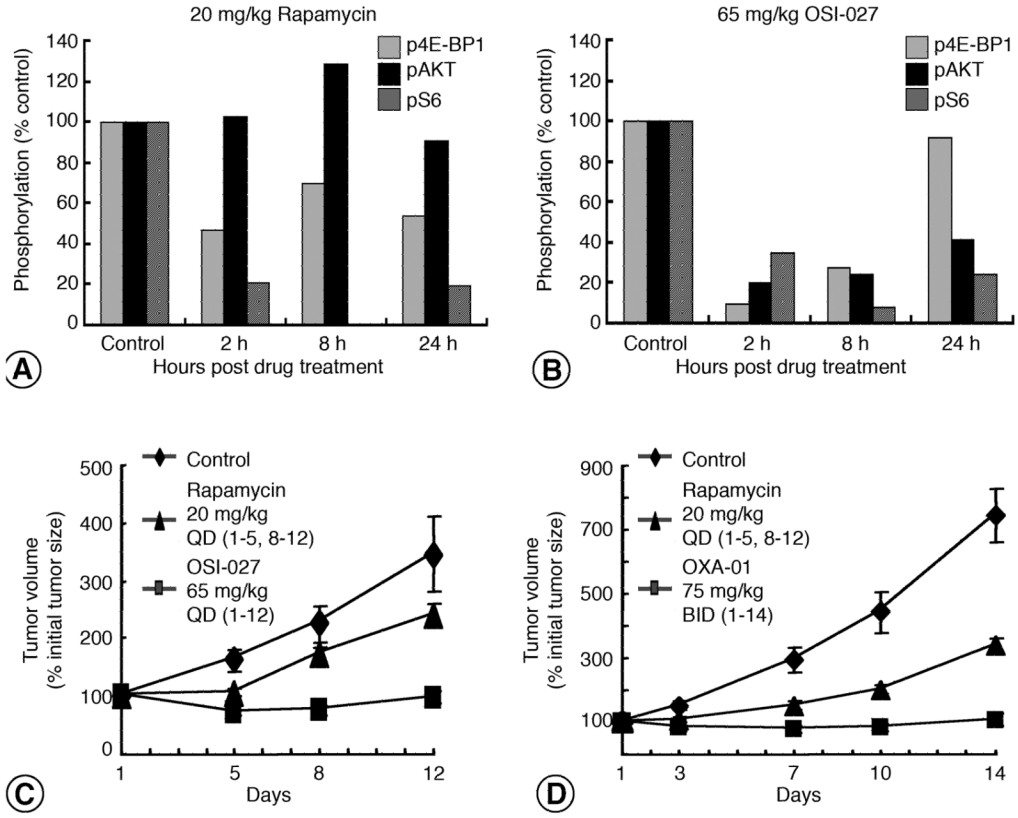

Figure 2. Effects of OSI-027, OXA-01, and rapamycin on tumor growth and pharmacodynamics

A. GEO tumors at 2, 8 and 24 hours after 12 days of rapamycin (20mg/kg) or vehicle treatment and effects on mTOR signaling were measured. Downstream effector phosphorylation of 4E-BP1 37/46 (light gray bars), Akt 473 (black bars), and S6 235/236 (dark gray bars) are shown (n=2). **B.** Mice bearing GEO xenografts were treated for 12 days with OSI-027 (65mg/kg) or vehicle and tumors collected at 2, 8, and 24 hours. Phosphorylation of mTOR signaling is shown (n=2). **C–D.** Mice bearing GEO xenograft tumors were treated with OSI-027 or rapamycin (**C)** or OXA-01 or rapamycin **(D)** and tumor volumes were plotted against time.

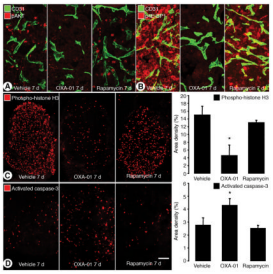

Figure 3. mTOR inhibition on downstream signaling, proliferation, and apoptosis of RIP-Tag2 tumors

A. Confocal images of tumor blood vessels (CD31; green) and phosphorylated-Akt (red) in RIP-Tag2 tumors after 7-day treatment of vehicle, OXA-01, or rapamycin. **B.** Fluorescent images of RIP-Tag2 tumors stained for tumor blood vessels (CD31; green) and phosphorylated-4E-BP1 after treatment. **C.** Phospho-histone-H3 (PHH3) staining and quantification in RIP-Tag2 tumors after vehicle, OXA-01 or rapamycin treatment for 7 days. **D.** Apoptotic cells stained with activated-caspase-3 in RIP-Tag2 tumors after a 7-day treatment. Scale bar in D represents 25μm in A and B; 100μm in C and D. *P<0.05 vs. all other groups.

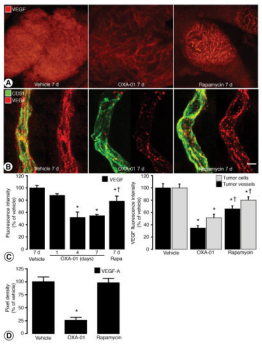

Figure 4. VEGF immunoreactivity with mTORC1/mTORC2 inhibition

A. Fluorescent images of RIP-Tag2 tumors stained for VEGF after 7-day treatment with vehicle, OXA-01, or rapamycin. **B.** High magnification confocal images of RIP-Tag2 tumor vessels (CD31; green) with associated VEGF (red) after treatment. **C.** Quantification of VEGF fluorescence intensity in the overall tumor (left) and within tumor cells versus tumor vessels (right). **D.** Pixel density of VEGF in RIP-Tag2 tumors treated with vehicle, OXA-01 or rapamycin detected with antibody arrays. Scale bar in B represents 100μm in A; 6μm in B. *P< 0.05 vs. vehicle. †P<0.05 vs. OXA-01.

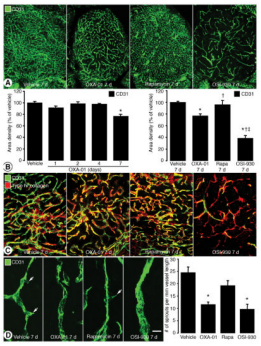

Figure 5. Effects of mTOR inhibition on tumor vessels

A. RIP-Tag2 tumor blood vessels (CD31; green) after treatment for 7 days. **B.** Time course quantifications of OXA-01 treatment on CD31 area density (left) and the comparison of 7-day treatment with vehicle, OXA-01, rapamycin (Rapa), and OSI-930 (right). **C.** Confocal images of RIP-Tag2 tumor blood vessels (CD31; green) and basement membrane (type IV collagen; red) after treatment for 7 days. **D.** Confocal images and quantification of tumor vessel sprouts after treatment for 7 days. Scale bar in D represents 100 μm in A; 50 μm in C; 12 μm in D. *P< 0.05 vs. vehicle. †P<0.05 vs. OXA-01. ‡P<0.05 vs. rapamycin.

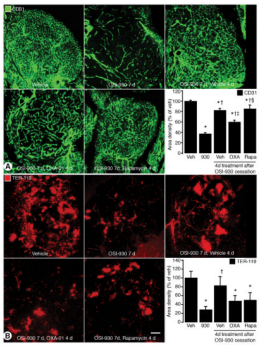

Figure 6. Effects of mTOR inhibition after cessation of VEGFR inhibition

A. Confocal images of tumor blood vessels (CD31; green) and quantification of CD31 area density are shown. **B.** Confocal images and quantification of the erythrocyte marker, TER-119 (red). Scale bar in B represents 100μm in A and B. *P<0.05 vs. vehicle. †P<0.05 vs. OSI-930. ‡P<0.05 vs. OSI-930 7d, Vehicle 4d. §P<0.05 vs. OSI-930 7d, OXA-01 4d.

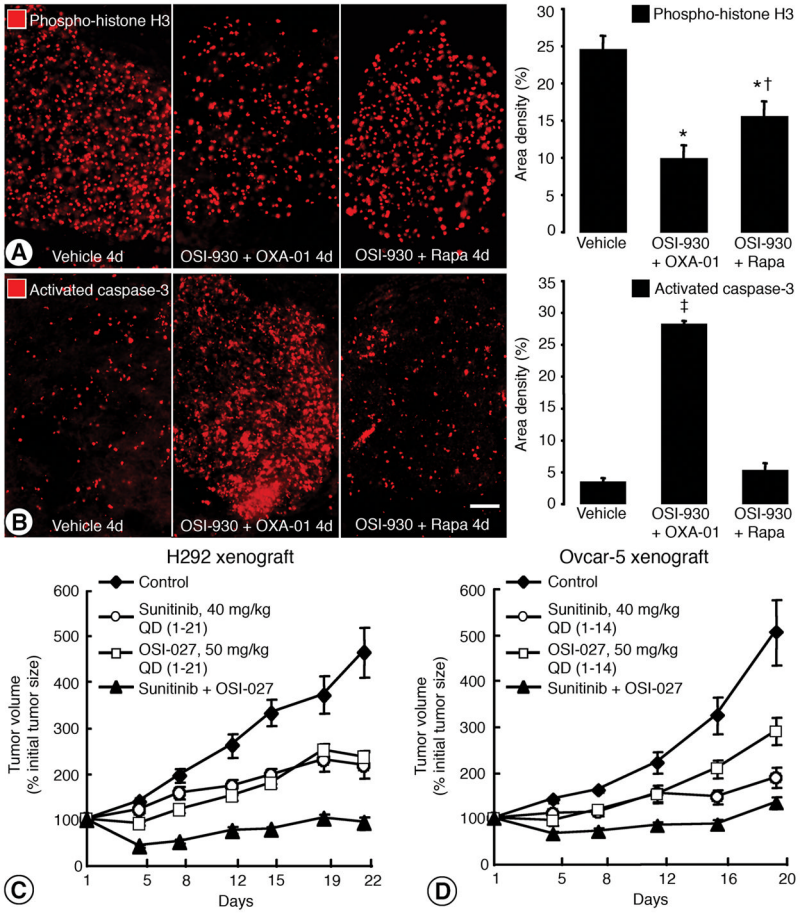

Figure 7. Anti-tumor effects of VEGFR2 plus mTORC1/2 inhibition

Confocal images and quantification of phospho-histone-H3 (**A**) and activated caspase-3 (**B**) are shown. Tumor growth of H292 lung cancer xenografts **(C)** and Ovcar-5 ovarian carcinoma xenografts **(D)** treated with vehicle, sunitinib (40 mg/kg), OSI-027 (50 mg/kg), or the combination of sunitinib and OSI-027. Scale bar in B represents 100μm in A and B. **P* < 0.05 vs. vehicle. †*P* < 0.05 vs. OSI-930 + OXA-01. ‡*P* < 0.05 vs. all other treatment groups.